BRITISH CERAMIC PROCEEDINGS

BETTER CERAMICS THROUGH PROCESSING

Edited by

J. Binner and J. Yeomans

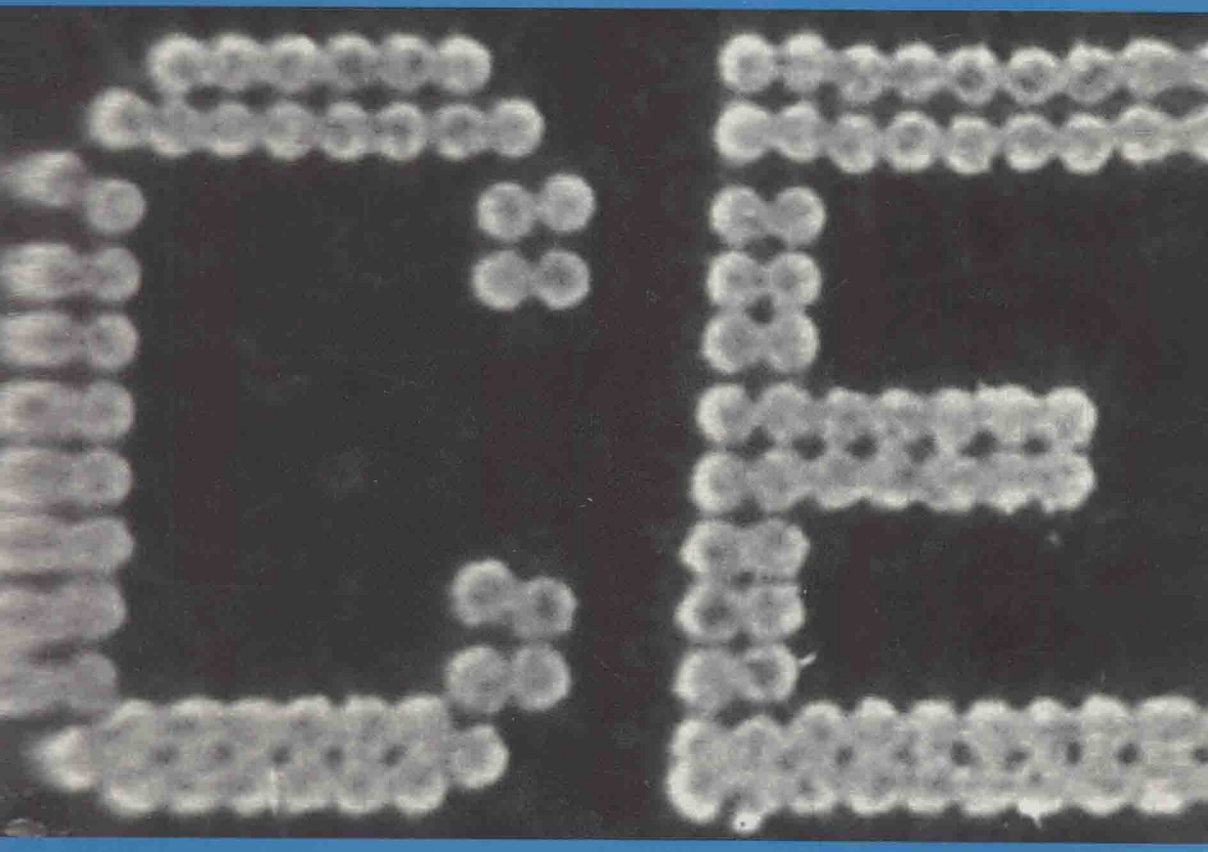

British Ceramics Proceedings
No. 58

BETTER CERAMICS THROUGH PROCESSING

Edited by

J. Binner
Department of Materials
Engineering and Materials Design
Faculty of Engineering
The University of Nottingham
University Park
Nottingham NG7 2RD

and

J. Yeomans
Department of Materials
Science and Engineering
The University of Surrey
Guildford GU2 5XH

British Ceramics Proceedings
No. 58

Book 674
Published in 1998 by
IOM Communications Ltd
1 Carlton House Terrace
London SW1Y 5DB

ISSN 0268–4373
ISBN 1 86125 033 9

IOM Communications Ltd
is a wholly-owned subsidiary of
The Institute of Materials

Typeset by
Fakenham Photosetting Ltd
Fakenham, UK

Printed and bound at
The University Press
Cambridge, UK

BRITISH CERAMICS PROCEEDINGS
NO. 58

BETTER CERAMICS THROUGH PROCESSING

Recent British Ceramic Proceedings

53 Novel Synthesis and Processing of Ceramics (1994)
Edited by F. R. Sale

54 Ceramic Films and Coatings (1995)
Edited by W. E. Lee

55 21st Century Ceramics (1996)
Edited by D. P. Thompson and H. Mandal

56 Ceramic Oxygen Ion Conductors
and Their Technological Applications (1996)
Edited by B. C. H. Steele

57 Advances in the Characterisation of Ceramics (1997)
Edited by R. Freer

Contents

Development and Evaluation of Alumina Calcination

IAN BENNETT and RON STEVENS
Department of Materials, University of Bath, Bath, UK

ABSTRACT

Much work has been performed on characterisation of intermediate phases during calcination and dehydration of various alumina hydrates. The most important factors found to affect transitions between the intermediate phases include the crystal size and morphology of the starting hydrate, the calcination conditions, including temperature, heating rate and atmosphere, and the amount of additives or impurities present.

In this work the calcination routes of three Gibbsites were investigated. The Gibbsites differ in their initial morphology and grain size. The calcined materials were characterised using XRD and SEM.

INTRODUCTION

Scientific investigation of alumina dates back to the nineteenth century,[1] with the first commercial application being reported in 1907. Alumina is today used as a raw material for refractory production, as an abrasive, in whiteware, in sparkplugs and in many other ceramic applications. Growth markets include advanced ceramics, catalysts and bio-materials.[2]

The bulk raw material for alumina production is bauxite.[3] Extraction is most commonly achieved by a wet alkaline process, known as the Bayer process. This involves the digestion of bauxite ore in hot-caustic soda followed by the precipitation under pressure of alumina using a seeding process involving a fine alumina hydroxide. Gibbsite is the usual precipitating phase, which is then washed and filtered. Phases other than Gibbsite can be produced using different processing conditions and alternative seeding crystals. Gibbsite can be used directly in the production of aluminium sulphate, as the polishing agent in toothpaste and in pharmaceutical products. It is also of increasing importance as a fire retardant filler, incorporated in other materials.

DEHYDRATION MECHANISMS

Dehydration of Gibbsite can take place via a number of distinct routes depending on the grain size and morphology of the starting material and the calcination conditions. It is also influenced by the presence of additives and impurities.[4]

In vacuum, Gibbsite has been found to transform via ρ, between 100 and 400°C, and ϵ, between 270 and 500°C, to α-alumina at 1150°C. In air, fine particle size Gibbsite transforms via χ, between 300 and 500°C, and κ, between 800 and 1150°C, to α-alumina. Coarse Gibbsite in air transforms both via χ and κ and via Boehmite, between 60 and 300°C, γ, between 500 and 850°C, and δ between 850 and 1050°C, followed by θ and

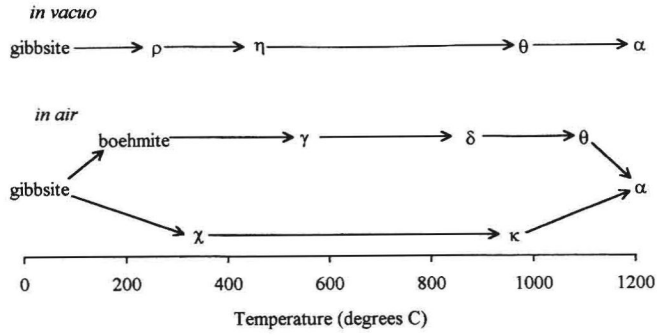

Figure 1. Thermal transformation sequences for Gibbsite (after Slade et al.).

α-alumina. The formation of the Boehmite phase is thought to be promoted by the presence of water vapour. In the coarse crystal the water released on dehydration cannot readily escape, leading to an increase in water vapour pressure within the crystal.[5,6] At high heating rates a reduced level of boehmite is found.[7] This is explained by the defective structure of the intermediates acting as pathways, allowing the water vapour to escape.

The transition temperatures between the phases are affected by the starting material, the particle size, the extent of disorder or activity of the material, gases in the calcining atmosphere, impurities and additives.

Gibbsite is a monoclinic α-alumina trihydrate. Boehmite is an orthorhombic α-alumina monohydrate. χ-Alumina has a cubic structure. γ-Alumina is considered to be cubic, but is sometimes taken as having a spinel structure. δ-Alumina has been identified as tetragonal or purely amorphous. κ-Alumina is an orthorhombic phase. α-Alumina is rhombohedral with a theoretical density of 3.96 to 3.98 g/cm.[3]

EXPERIMENTAL

Dehydration experiments were performed on three different Gibbsites. Gibbsite A has a particle size of approximately 38 μm with a small fraction of the particles below 1 μm. It is made up of agglomerates of angular crystals with smooth surfaces. Optical cross-sections show an agglomerated core with radial growth from the core to the surface. Gibbsite B has a particle size of approximately 62 μm. It is again made up of agglomerates of angular crystals (Fig. 2). It has less smooth surfaces than A with some cracking along crystal planes. Optical cross-sections show more obvious radial growth from a smaller agglomerated core than in the case of A (Fig. 3). Gibbsite C has a particle size of approximately 127 μm. It is made up of agglomerates of crystals rounded off at the surface of the agglomerates. Cross-sections again showed radial growth with little or no agglomerated core. XRD showed all three materials to be single-phase crystalline Gibbsite.

The materials were heated at 60°C/hour up to 200, 400, 600, 800, 1000 and 1200°C. They were held at that temperature for one hour and then allowed to cool. The weight of the

Figure 2. SEM of Gibbsite B as received.

powder was measured before and after dehydration. The resulting powders were studied using XRD and SEM.

RESULTS

At 200°C little change was seen in the XRD pattern when compared to the starting materials. Certain of the Gibbsite peaks are somewhat less intense though not significantly. A weight loss of 1 to 2% is measured for all materials. This can be attributed to evaporation of any moisture not incorporated in the hydrate structure. These observations are in agreement with those found in the literature. Longer heating times, of the order of hundreds of hours, have resulted in the formation of monohydrates, but when a holding time of 1 hour is used, little change is expected.

At 400°C all materials show a Boehmite phase with the background to peak ratio for A marginally greater than for the others. A, has the finest particle size which should result in a reduced level of Boehmite formation. All the materials show a 19–20% weight loss with respect to their starting weights. This correlates to the loss of 2 moles of water for each Al_2O_3 molecule when starting with the trihydrate, indicating the presence of a monohydrate.

At 600°C all powders show both γ and χ phases with a high background to peak ratio and

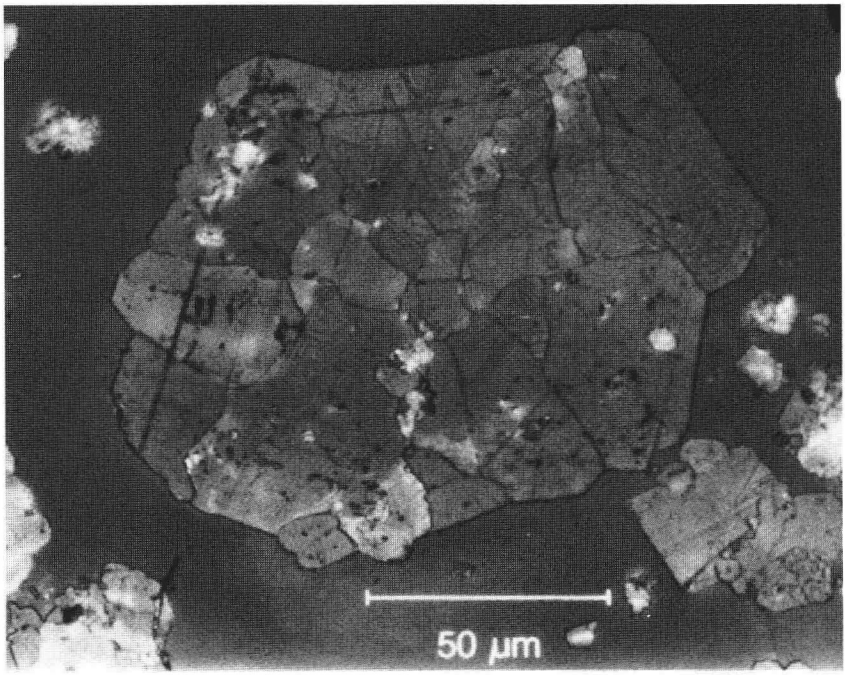

Figure 3. Optical cross-section of Gibbsite B as received

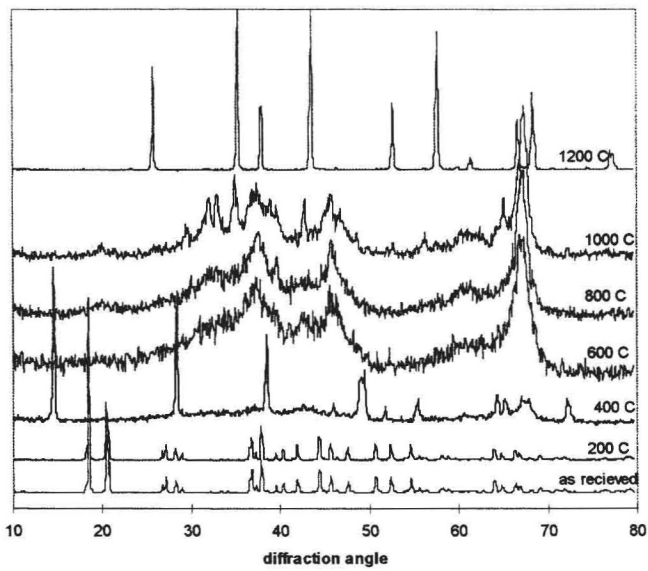

Figure 4. XRD of Gibbsite B showing phase changes during calcination up to 1200°C

many of the peaks not clearly defined. The presence of both phases indicates a combination of the dehydration routes reported in the literature for coarse Gibbsites calcined in air. Weight loss of 26 to 29% was measured, indicating that most of the hydrate had transformed to an anhydrous form of alumina.

At 800°C the γ and χ phases are more clearly defined for all the powders. The weight loss of 30 to 33% indicates that almost total transformation of the hydrate has taken place at this temperature. An increased amount of laminar surface cracking is seen in material B when sintering at this and higher temperatures.

At 1000°C all materials show a κ phase. The δ phase may also be present, but this form may be hard to identify using XRD as it produces a weak X-ray pattern in comparison to the κ phase. Weight loss of 32 to 34% indicates near complete dehydration of the hydrate to anhydrous alumina.

At 1200°C a single-phase, crystalline α-alumina is seen in all cases with no discernible evidence for other crystalline forms. Weight loss in excess of 35% indicates complete transformation of the hydrate to anhydrous alumina within the one hour holding time at this temperature. From SEM micrographs grain growth is seen for all materials relative to the materials calcined at the lower temperatures. Laminar surface cracking is observed in material A as well as in B at this temperature, with little or no change in the surface morphology of material C.

DISCUSSION

The presence of both the Boehmite and γ phases and the χ and κ phases would indicate a dehydration route comparable to those cited from the literature for coarse Gibbsites in air.

The phases found to be present at the various temperatures correspond well with those reported in the literature. Some of the reported phases have not been observed. In the case of δ-alumina this may be due to a weak X-ray pattern relative to the κ phase which is present in the same calcination temperature range. θ-Alumina is reported in the literature at temperatures above 1000°C, but below 1200°C. This would explain why it has not been observed in these experiments. Further experiments are required to determine more precisely the transformation temperatures, with longer holding times needed to allow the phases present to develop more completely to the equilibrium state.

The surface cracking in Gibbsites A and B may be due to the accommodation of the volume change due to the loss of water on dehydration. The absence of significant cracking in Gibbsite C may be due to the radial crystal growth allowing more easy accommodation of the loss of water.

Other investigations in addition to those discussed above include a study of the influence of additives on the transformation route and temperatures at which the transformations take place. In particular, the effect of fluorides on the transformation temperatures and the morphology of the intermediate phases has been considered significant. Fluorides can reduce the transformation temperatures so reducing the cost of the process, but their presence also leads to the growth of very platy crystals.[8] A better understanding of the complex mechanisms involved allowing greater control over the crystal growth and morphology is desirable.

The possibility of a mechanical pre-treatment of the Gibbsite will also need to be considered. Phase changes and reductions in transformation temperatures have been achieved by high-impact milling of various alumina phases.[9,10] Limited success with this process has been reported, with further work necessary to determine the critical parameters.

CONCLUSIONS

The presence of Boehmite on calcination of all three Gibbsites indicates that they all fall into the coarse grained category as defined by previous authors. Differences in the agglomerate structure lead to some differences in the surface structure of the calcined aluminas.

Further work will concentrate on finding a suitable additive or combination of additives, allowing a reduction in transformation temperature to α-alumina, whilst generating a morphology suited to further processing. The use of fluoride to reduce the transformation temperature, in combination with a surface stabiliser, may allow this objective to be achieved.

REFERENCES

1. E. Dorre and H. Hubner: 'Alumina', 1984, Springer Verlag.
2. G. MacZura, K. J. Moody and J. T. Tyson: *Ceram. Bull.*, **70**(5), 846–848.
3. 'An Introduction to Alumina ... ', The British Alumina Company Ltd.
4. W. H Gitzen: 'Alumina as a Ceramic Material', 1970, The American Ceramic Society.
5. J. H. de Boer, J. M. H. Fortuin and J. J. Steggerda: *Proc. Kon. Ned. Ak. Wet.*, 1954, **B17**, 170–179.
6. J. H. de Boer, J. M. H. Fortuin and J. J. Steggerda: *Proc. Kon. Ned. Ak. Wet.*, 1954, **B57**, 434–447.
7. K. Yamada et al.: in 'Light Metals', 1984, ed. J. P. McGeer, Metall. Soc. AIME.
8. C. A. Shaklee and G. L. Messing: *J. Am. Ceram. Soc.*, **77**(11), 2977–2984.
9. P. A. Zielinski et al.: *J Mater. Res.*, **8**(11), 2985–2992.
10. J. Ding, T. Tsuzuki and P.G. McCormick: *J. Am. Ceram. Soc.*, **79**(11), 2956–2958.

The Preparation of Ce α-Sialons and Related Unstable Phases

D. P. THOMPSON* and H. MANDAL†

† *Department of Ceramic Engineering, Anadolu University, 26370 Eskisehir, Turkey.*

and

* *Materials Division, Department of Mechanical, Materials & Manufacturing Engineering, University of Newcastle upon Tyne, UK*

ABSTRACT

It has previously been accepted that lanthanum and cerium do not form α-sialon structures because their ions are too large to enter the interstices in the structure. Recent work on heat-treatment of rare-earth densified α- and mixed α-β sialons has shown that many α-sialon compositions prepared by sintering at 1750–1800°C are unstable at lower (1300–1600°C) temperatures. This instability is dependent on α-sialon composition, and is more marked for α-sialons prepared using low rather than high atomic number rare earths. An important requirement of such studies is rapid quenching of the initial sintered sample in order to prevent decomposition of the α-sialon phase during cooling. The present work demonstrates that cerium stabilised α-sialon is in fact stable at sintering temperatures and that this phase has not been observed previously because under normal cooling rates the α-phase totally transforms to β-sialon (plus glass) on cooling. Similar phenomena are discussed in the case of Nd_2O_3-densified sialons, where a fine-grain size β-sialon matrix can be observed by decomposition of an α-sialon phase initially formed at sintering temperatures. $\alpha \rightleftarrows \beta$ transformation provides a useful processing variable for optimising the microstructure and hence the mechanical properties of β- and mixed α-β sialon ceramics.

1. INTRODUCTION

It is widely assumed in silicon nitride processing that the product assemblage at firing temperatures is preserved on cooling down to room temperature, but with minor changes to secondary phases e.g. liquid crystallisation or conversion into a glass. This is based on the related assumption that the high temperature products are equilibrium phases under the given experimental conditions, and phases that are stable at high temperatures, are normally also stable at room temperature. However, this is not a universal truth, and systems do exist in which phase transformations occur on cooling. These transformations are generally not easy to observe because no characterisation work is carried out at high temperatures; when it is established that they do take place, the resulting material offers the unique possibility of microstructural tailoring, because subsequent heat-treatment can be used to develop an optimum microstructure with desired mechanical properties.

α-sialons are well-established compounds, with the general formula $M_xSi_{12-m-n}Al_{m+n}O_nN_{16-n}$,[1] where M is one of the cations Li, Mg, Ca, Y and most rare earths (excluding La, Eu), m is the number of Si-N bonds in α-Si_3N_4 replaced by Al-N, n is the number of Si-N bonds in α-Si_3N_4 replaced by Al-O, and x is equal to m divided by the valency of the M cation. Recent work[2–12] has shown that most rare earth α-sialons transform to β-sialon plus other crystalline or vitreous phases, when heat-treated in the

temperature range 1300–1600°C. The ease with which this transformation proceeds decreases with increasing atomic number of the rare earth cation; indeed, in the absence of β-sialon nuclei, certain ytterbium α-sialon compositions do not transform to β even when high levels of liquid phase are present.[13] When α-sialon ceramics are prepared by firing at temperatures in the range 1750–1800°C, some α→β transformation occurs on cooling through the temperature range 1300–1600°C. Under normal cooling rates (i.e. switching off the power to the furnace), the cooling rate is determined by the size of the furnace, and generally results in total transformation to β for low-Z samples cooled in large industrial furnaces; more modest levels of transformation occur in small laboratory furnaces. Obviously in order to study the transformation in detail, it is important to *quench* compositions from the sintering temperature down to room temperature (this also has the advantage of minimising the amount of crystallisation of grain boundary glassy phase) and then to promote α→β transformation in a subsequent heat-treatment step. In the case of Li-, Mg- and Ca- α-sialons, no α→β transformation has been observed; however, a relatively limited amount of experimental work has been carried out in these systems.[14]

The present paper is concerned with the stability of low atomic number rare earth α-sialons. It is well established that a pure lanthanum α-sialon phase does not occur, and prior to the present work it was accepted that Ce α-sialons were also unstable (even though Ce could enter into an α-sialon structure if it was also accompanied by a smaller cation e.g. Y^{3+}.[15,16] Neodymium α-sialons have been prepared, but it was generally believed, that the occurrence of a melilite phase ($Nd_2Si_{3+x}Al_xO_{3+x}N_{4-x}$, $0 < x < 1$)) in this system reduced the amount of neodymium α-sialon observed. It is now known that these compositions are often pure α-sialon at firing temperatures, but transform to β-sialon (plus other phases, e.g. melilite) during cooling to room temperature. The present paper discusses these results, and indicates how they can be used to obtain controlled sialon microstructures with improved mechanical properties.

2. EXPERIMENTAL

In the present work, α-sialon compositions were prepared by hot-pressing using CeO_2 and Nd_2O_3 as the rare earth oxides. The resulting materials were rapidly cooled and then heat-treated in the temperature range 1350–1625°C to allow α→β transformation (and other associated reactions) to occur. The resulting materials were characterised by X-ray diffraction and by scanning electron microscopy.

Mixed powders of Si_3N_4 (H. C. Starck-Berlin, Grade LC10), AlN (H. C. Starck-Berlin, Grade A), Al_2O_3 (Alcoa, Grade A16SG) together with CeO_2 or Nd_2O_3 as the densifying additive to give an overall α-sialon composition $Ln_{0.5}Si_9Al_3O_{1.5}N_{14.5}$ (i.e. $m = n = 1.5$ in the general α-sialon formula quoted above), were wet-mixed in isopropanol, dried and compacted into pellets by uniaxial and then isostatic pressing at 200 MPa. Before firing, the specimens were embedded in fine boron nitride powder in graphite dies, and hot-pressed at 1800°C for 1 h. Since some α→β transformation and grain-boundary crystallisation/devitrification always occurred during cooling after hot-pressing,[2] samples were placed in a carbon crucible and re-heated to 1800°C in a small pressureless sintering furnace for 15 minutes, quenched (600°C/min) to 1100°C and then cooled to room temperature

(300°C/min). Heat-treatment was subsequently carried out in an alumina tube furnace for either 24 h at 1350 or 1450°C, or for 8 h at 1625°C under a nitrogen gas atmosphere.

Phase identification was carried out using a Hägg–Guinier focusing X-ray camera and $CuK\alpha_1$ radiation. The computer-linked scanner (SCANPI LS-20) system developed by Werner (Stockholm University) was used for direct measurement of X-ray films. The amounts of α- and β-sialon phases were established by the method given by Liddell.[17] Microstructures were observed using a Camscan S4-8ODV scanning electron microscope equipped with a windowless energy dispersive X-ray analyser (EDX).

3. RESULTS AND DISCUSSION

The composition m = 1.5, n = 1.5 was selected for study because this is close to the minimum oxygen limit of α-sialon compositions for easy investigation (i.e. excluding the use of LnN as starting compounds because of their expense and sensitivity to hydrolysis); also a recent study had focused on these compositions for a range of rare earth α-sialons.[11]

3.1 Ce α-sialons

X-ray examination of m = n = 1.5 Ce α-sialon samples hot-pressed at 1800°C, re-sintered and quenched, indicated 20% of α-sialon and 80% of β-sialon with a trace of 21R phase. The measured density of the sample was found to be 3.403 gcm^{-3}, and SEM examination of polished cross-sections showed no porosity, indicating that the sample had reached virtually theoretical density by hot-pressing. Typical microstructures for sintered samples after rapid cooling are shown in Fig. 1. Back-scattered micrographs very clearly distinguish between β-sialon and 21R (both black, acicular grains containing no Ce), α-sialon (grey, small Ce content) and the fine-grained dispersion of grain-boundary glass (white, with a high Ce content). EDX spectra (Fig. 2) also allow β-sialon (a) and α-sialon (b) grains to be distinguished on the basis of Ce content, but in addition the β ($\approx Si_5AlON_7$) and 21R ($SiAl_6O_2N_6$) (c) grains can be distinguished by Si:Al ratio. The slight Ce signal from β-sialon grains is believed to arise because of beam penetration into adjacent glassy regions.

The higher magnification picture shown in Fig. 1(b) brings out more clearly the α-sialon grains in the microstructure. They tend to occur in small clumps, surrounded by a fine-grained dispersion of more equiaxed β grains + glass pockets, with the larger β needles interspersed here and there. The grains have well-defined crystalline morphologies, with a tendency to form as needles of low aspect ratio.

Heat-treatment of samples was carried out at the three different temperatures 1350, 1450 and 1625°C. In each case, the samples were quenched back to room temperature after heat-treatment. As can be seen from Table 1, only 5% of α-sialon was retained after heat-treatment at 1350°C; β-sialon was the sole crystalline product after heat-treatment at the other two temperatures.

$CeAlO_3$ easily devitrifies out of grain boundary glasses in sialon ceramics at 1350°C, and

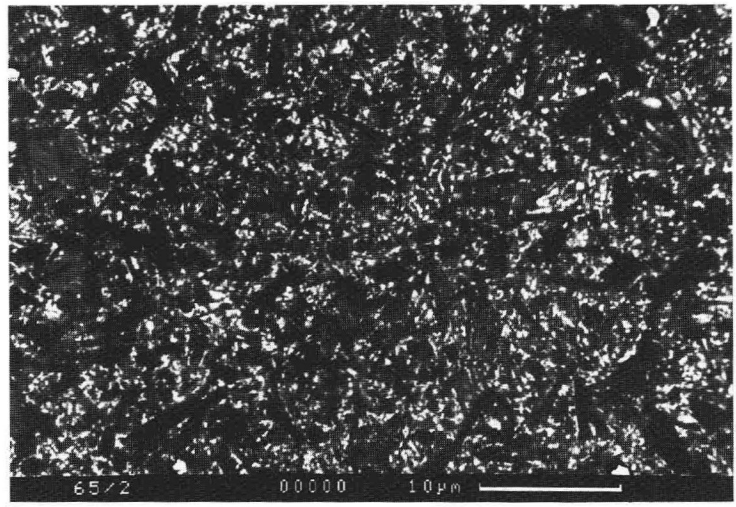

(a)

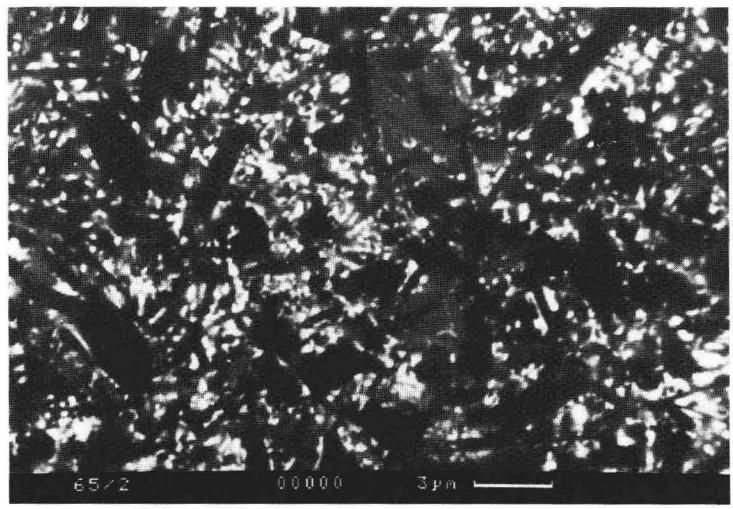

(b)

Figure 1. Micrographs of m = 1.5, n = 1.5 Ce α-sialon, (a) × 2250 and (b) × 4500.

Table 1. X-ray diffraction results of heat-treated samples

T (°C)	t (h)	α' (%)	β' (%)	Others
As-sintered		20	80	21R(w)
1350	24	5	95	21R(m), $CeAlO_3$(mw)
1450	24	0	100	21R(mw), JEM(w)
1625	8	0	100	21R(w), JEM(ms)

s, m, w = strong, medium, weak etc.; JEM = $CeSi_5Al_2ON_9$.[18,19]